

## Structural Role of Hydration Water in Na- and H-Magadiite: A Spectroscopic Study

Céline Eypert-Blaison,<sup>\*,†</sup> Bernard Humbert,<sup>‡</sup> Laurent J. Michot,<sup>†</sup>  
Manuel Pelletier,<sup>†</sup> Emmanuel Sauzéat,<sup>†</sup> and Frédéric Villieras<sup>†</sup>

Laboratoire Environnement et Minéralurgie, INPL-ENSG-CNRS UMR 7569, BP 40,  
54501 Vandoeuvre Cedex, France, and Laboratoire de Chimie Physique Pour l'Environnement,  
UMR CNRS-UHP, Nancy I 7564, France

Received October 23, 2000. Revised Manuscript Received February 7, 2001

The layered silicic acid H-magadiite and the corresponding Na<sup>+</sup> salt have been investigated by a combination of three spectroscopies: <sup>29</sup>Si nuclear magnetic resonance, infrared absorption, and Raman scattering. When sodium ions are exchanged with protons, the resulting H-magadiite does not swell any more and displays a less crystalline structure than the corresponding Na sample. Similar low crystallinity is also observed in fully dehydrated Na-magadiite samples, which clearly reveals that water molecules play a crucial structural role for local ordering, which must be taken into account. Indeed, by combining three spectroscopic techniques under various hydration conditions, several vibrations bands of the silicate layers can be assigned precisely, leading to refined structural information. In particular, assignments in the spectral region corresponding to the vibrations of silicate layers reveal three hydration states that can be correlated to previous observations on the stretching and bending OH vibrations, which evidenced three distinct organizations of adsorbed water molecules.

### Introduction

Magadiite is a natural crystalline hydrated sodium silicate<sup>1</sup> which can be easily synthesized.<sup>2–4</sup> It is a layered structure with an ideal unit cell of Na<sub>2</sub>Si<sub>14</sub>O<sub>29</sub>·xH<sub>2</sub>O<sup>1,2,5</sup> containing terminal oxygen atoms neutralized by Na<sup>+</sup> ions. Upon acid treatment, these sodium ions can be ion-exchanged with protons to form the crystalline silicic H-magadiite,<sup>1,5–7</sup> which formula was reported by Lagaly and co-workers as H<sub>2</sub>Si<sub>14</sub>O<sub>29</sub>·5.4H<sub>2</sub>O. Na-magadiite exhibits some of the classical properties of charged layered materials<sup>8,9</sup> such as interlamellar sorption of water and polar organic molecules<sup>6</sup> and cation exchange of internal surface cations. These properties could promote its application as cation exchanger,<sup>10</sup> adsorbent,<sup>11,12</sup> or catalyst.<sup>6</sup> In the case of H-magadiite,

the surface silanol groups, first described by Rojo et al.,<sup>7</sup> can react with a large number of organic compounds to form intercalated complexes.<sup>6</sup> These organic swelling complexes of magadiite can then be used as precursors for pillaring reactions.<sup>13–15</sup>

Knowing the exact structure of these minerals would certainly provide useful information for tailoring their chemical properties. Unfortunately, the small dimensions of single crystals of natural and synthetic magadiite preclude the use of X-ray diffraction (XRD) techniques for establishing the structure of this mineral.<sup>5,16</sup> Spectroscopic techniques have thus been extensively used in the past two decades for trying to obtain detailed structural information on both Na- and H-magadiite. High-resolution solid-state <sup>29</sup>Si magic angle spinning–nuclear magnetic resonance (MAS NMR) is well-suited for elucidating the structure of zeolites and other silicates.<sup>17–19</sup> Schwiieger and co-workers were then the first to use this technique for studying the structure of silicate layers in three synthetic sodium silicate hy-

\* To whom correspondence should be addressed.

<sup>†</sup> Laboratoire Environnement et Minéralurgie.

<sup>‡</sup> Laboratoire de Chimie Physique pour l'Environnement.

(1) Eugster, H. P. *Science* **1967**, *157*, 1177.

(2) Lagaly, G.; Beneke, K.; Weiss, A. *Am. Miner.* **1975**, *60*, 642.

(3) Schwiieger, W.; Heidemann, D.; Bergk, K. H. *Rev. Chim. Miner.* **1985**, *22*, 639.

(4) Fletcher, R. A.; Bibby, D. M. *Clays Clay Miner.* **1987**, *35*, 318.

(5) Brindley, G. W. *Am. Miner.* **1969**, *54*, 1583.

(6) Lagaly, G.; Beneke, K.; Weiss, A. *Am. Miner.* **1975**, *60*, 650.

(7) Rojo, J. M.; Ruiz-Hitzky, E.; Sanz, J.; Serratos, J. M. *Rev. Chim. Miner.* **1983**, *20*, 807.

(8) Pinnavaia, T. J. *Science* **1983**, *220*, 365.

(9) Kim, C. S.; Yates, D. M.; Heaney, P. J. *Clays Clay Miner.* **1997**,

*45*, 881.

(10) Wolf, F.; Schwiieger, W. *Z. Allg. Anorg. Chem.* **1979**, *457*, 224.

(11) Jeong, S. Y.; Lee, J. M. *Bull. Korean Chem. Soc.* **1998**, *19*, 218.

(12) Fudala, A.; Kiyozumi, Y.; Mizukami, F.; Toba, M.; Niwa, S. I.; Kiricsi, I. *J. Mol. Struct.* **1999**, *482*, 43.

(13) Ruiz-Hitzky, E.; Rojo, J. M.; Lagaly, G. *Colloid Polymer Sci.* **1985**, *263*, 1025.

(14) Sprung, R.; Davis, M. E.; Kauffman, J. S.; Dybowski, C. *Ind. Eng. Chem. Res.* **1990**, *29*, 213.

(15) Dailey, J. S.; Pinnavaia, T. J. *Chem. Mater.* **1992**, *4*, 855.

(16) Brandt, A.; Schwiieger, W.; Bergk, K. H. *Rev. Chim. Miner.* **1987**, *24*, 564.

(17) Lippmaa, E.; Mägi, M.; Samoson, A.; Engelhardt, G.; Grimmer, A. R. *J. Am. Chem. Soc.* **1980**, *102*, 4889.

drates with various SiO<sub>2</sub>/Na<sub>2</sub>O molar ratios: octosilicate, magadiite, and kenyaite.<sup>3</sup> For each of the studied samples, only Q<sup>3</sup> and Q<sup>4</sup> signals were observed, and a correlation between the intensities of these two NMR signals with the SiO<sub>2</sub>/Na<sub>2</sub>O molar ratio was evidenced. Based on this correlation, a model representation was proposed assuming that each layered silicate hydrate can be formed from the condensation of makatite layers of known crystal structure. Such structural interpretation is similar to a previous model proposed by Annahed et al.,<sup>20</sup> on the basis of XRD results. However, the structural formula deduced by using such a model were not in agreement with the experimental ones. Such discrepancy was attributed to variations in the water contents of those minerals. This model was then refined by Brandt et al.,<sup>16</sup> but the resulting structure still does not fit all the data observed for magadiite. Using the same spectroscopic technique, Pinnavaia et al. studied the structural compositions of the layered silicic acid H-magadiite and the corresponding Na<sup>+</sup> salt.<sup>21</sup> Both exhibits Q<sup>3</sup> and Q<sup>4</sup> signals, with a Q<sup>3</sup>:Q<sup>4</sup> site ratio of 1:3. The anhydrous layered structure proposed to explain such observations consisted of five planes of atomic oxygen, with layers arising from double sheets of Q<sup>4</sup> tetrahedra with 25% of the tetrahedra "inverted" to form Q<sup>3</sup> units. <sup>1</sup>H<sup>7,22–24</sup> and <sup>23</sup>Na<sup>25,26</sup> NMR studies were also published. By comparing data from <sup>29</sup>Si, <sup>1</sup>H, and <sup>23</sup>Na NMR, Almond and co-workers proposed a new model in which kanemite, octosilicate, magadiite, and kenyaite structures could be derived from the known structures of anhydrous KHSi<sub>2</sub>O<sub>5</sub> and piperazine silicate (EU19).<sup>24</sup> However, such a model fails to provide a clear picture for magadiite and kenyaite as the <sup>29</sup>Si NMR spectrum of these two minerals cannot be explained properly on the basis of the structures of anhydrous KHSi<sub>2</sub>O<sub>5</sub> and piperazine silicate. Garcès et al. based their analysis of magadiite on an analogy with the structure of the zeolite dachiardite, supported by both infrared (IR) and <sup>29</sup>Si NMR data.<sup>27</sup> The resulting structural model consists of layers of six-membered rings of tetrahedra and blocks containing five-membered rings attached to both sides of the layers. This latter structural model was recently partially supported by Huang and co-workers based on a combined IR and Raman study.<sup>28</sup> In agreement with Garcès et al.,<sup>27</sup> they proposed a multilayer structure with five- and six-membered rings. However, their data also lead them to postulate the presence of additional Si–O–Si linkages with very large bond angles near

180°. In view of their failure, several authors<sup>3,21,24</sup> concluded on the essential role of water in the structure. Still, detailed studies of water in magadiite are rather scarce in the literature. Brandt et al. studied the thermal behavior of Na-magadiite, for temperatures ranging between 293 and 573 K, by combining XRD, differential thermal analysis, dilatometry, differential scanning calorimetry, and thermogravimetric measurements and revealed distinct steps in the dehydration of Na-magadiite.<sup>29</sup> Rojo et al. also used thermal treatments for investigating the evolution of the water signals of Na- and H-magadiite using IR and <sup>1</sup>H NMR spectroscopy.<sup>7,22</sup> On the basis of IR spectra of Na- and H-magadiite in regions from 4000 to 2500 cm<sup>-1</sup> (water stretching) and 1800 to 1400 cm<sup>-1</sup> (water bending) combined with <sup>1</sup>H NMR results, they suggested the presence of two distinct types of hydroxyl groups: OH groups involved in relatively strong hydrogen bonds between adjacent layers and "free" OH groups, probably pointing to holes of the next layers. In such a scheme, upon proton exchange, the silicic structure collapses through formation of hydrogen bonds between adjacent layers, then preventing interlayer adsorption of water molecules in H-magadiite.

We recently combined thermal analyses, water adsorption gravimetry, XRD, and IR measurements under controlled water pressure to investigate thoroughly the hydration and swelling behavior of Na-magadiite.<sup>30</sup> We evidenced that water adsorption occurs in three main steps. Infrared spectra recorded under various water pressures show distinct water populations. For relative pressures ≥ 0.20, some water molecules (1665 cm<sup>-1</sup>) are doubly hydrogen bonded, likely to surface sites, whereas others (1625 cm<sup>-1</sup>) exhibit a signal similar to that observed for hydrated clay minerals at low relative pressures, suggesting a strong influence of the interlayer cation. For lower relative pressures a single water population at 1635 cm<sup>-1</sup> is observed, suggesting a dual influence of both the interlayer cation and the surface sites. Such understanding of the evolution of water populations upon increasing water contents provides a sound base for studying the induced structural modifications of the silicate framework. In the present paper, we describe the results obtained on magadiite by combining <sup>29</sup>Si NMR, infrared, and Raman experiments. IR experiments were carried out for various water relative pressures upon water desorption, whereas the influence of water content for NMR and Raman studies was investigated by carrying out experiments under ambient atmosphere and under various vacuum conditions. In parallel to Na-magadiite, we also studied the proton-exchanged form, as H-magadiite exhibits a totally different swelling behavior. The comparison between these two samples should then provide valuable information about the links between water status and structural features of those sheet silicates.

## Experimental Section

Na-magadiite was prepared by reacting silica gel with aqueous NaOH according to previously described methods.<sup>30,41</sup>

(18) Lippmaa, E.; Mägi, M.; Samoson, A.; Tarmsak, M.; Engelhardt, G. *J. Am. Chem. Soc.* **1981**, *103*, 4992.

(19) Hater, W.; Müller-Warmuth, W.; Meier, M.; Frischat, G. H. *J. Non Cryst. Solids* **1989**, *113*, 210.

(20) Annahed, H.; Fälth, L.; Lincoln, F. J. *Z. Kristallogr.* **1982**, *159*, 203.

(21) Pinnavaia, T. J.; Johnson, I. D.; Lipsicas, M. *J. Solid State Chem.* **1986**, *63*, 118.

(22) Rojo, J. M.; Ruiz-Hitzky, E.; Sanz, J. *J. Inorg. Chem.* **1988**, *27*, 2785.

(23) Almond, G. G.; Harris, R. K.; Graham, P. *J. Chem. Soc., Chem. Commun.* **1994**, 851.

(24) Almond, G. G.; Harris, R. K.; Franklin, K. R. *J. Mater. Chem.* **1997**, *7*, 681.

(25) Almond, G. G.; Harris, R. K.; Franklin, K. R.; Graham, P. *J. Mater. Chem.* **1996**, *6*, 843.

(26) Hanaya, M.; Harris, R. K. *J. Mater. Chem.* **1998**, *8*, 1073.

(27) Garcès, J. M.; Rocke, S. C.; Crowder, C. E.; Hasha, D. L. *Clays Clay Miner.* **1988**, *36*, 409.

(28) Huang, Y.; Jiang, Z.; Schwieger, W. *Chem. Mater.* **1999**, *11*, 1210.

(29) Brandt, A.; Schwieger, W.; Bergk, K. H.; Grabner, P.; Porsch, M. *Cryst. Res. Technol.* **1989**, *24*, 47.

(30) Eypert-Blaison, C.; Sauzéat, E.; Pelletier, M.; Michot, L. J.; Villieras, F.; Humbert, B. *Chem. Mater.* **2001**, *13*, 1480.

H-magadiite was obtained by a slowly potentiometric titration with aqueous HCl of the Na-magadiite, and the final product was air-dried. The X-ray powder diffraction patterns and basal spacings (15.5 Å for Na-magadiite and 11.8 Å for H-magadiite) were in agreement with those previously reported for these minerals.<sup>5–7</sup> According to chemical and thermal analyses,<sup>30</sup> the unit cell formula of Na-magadiite can be written as  $\text{Na}_{2.07}\text{H}_{1.93}\text{Si}_{14}\text{O}_{30}\cdot 8.27\text{H}_2\text{O}$  and that of H-magadiite as  $\text{H}_4\text{Si}_{14}\text{O}_{30}\cdot 0.5\text{H}_2\text{O}$ .

Water vapor gravimetric adsorption experiments were carried out by using a lab-built quasi-equilibrium setup designed around a Setaram MTB 10–8 symmetrical microbalance. Water vapor was supplied to the sample (thermostated at 30 °C) from a source kept at 41 °C, at a slow flow rate to ensure quasi-equilibrium conditions at all times. The simultaneous recording of mass uptake and equilibrium pressure directly yields the water vapor adsorption isotherm. The experimental conditions were a sample mass of 105 mg and an outgassing at 50 °C during 18 h under a residual pressure of 1 Pa.

The <sup>29</sup>Si NMR spectra were recorded in a  $B_0 = 7$  T field at 59.62 MHz on a Bruker MSL 300 solid-state high-resolution NMR spectrometer. Samples were placed into 7-mm rotors and spun at 2000 Hz. Spectra were obtained from a single pulse excitation (pulse widths 3.9 μs with 400 scans) and by cross-polarization (CP; single contact time with 6 ms and 10 000 scans). The <sup>29</sup>Si chemical shifts were reported in parts per million (ppm) relative to tetramethylsilane. The sample examined under vacuum was prepared by outgassing at 50 °C during 18 h under a residual pressure of 1 Pa. It was then packed into a rotor inside a glovebox, sealed, and subsequently analyzed by NMR.

IR spectra were recorded by using an IR transmission cell specially designed for investigating the first hydration states of clay minerals.<sup>31</sup> The temperature and moisture of the sample are controlled. For these experiments, a magadiite film was prepared by depositing a few drops of a dilute aqueous suspension onto a ZnSe slide. The film is kept at  $30 \pm 0.1$  °C. The relative water vapor pressure is controlled in the cell in a  $P/P_0$  range between 0.01 and 0.85 by setting the temperature of a water source between  $-29$  and  $+27.2 \pm 0.1$  °C. The cell is equipped with ZnSe windows. The FT-IR spectra were recorded on a Bruker FT-IR spectrometer by using a DTGS detector. The IR spectra consisted of 100 averaged scans in the range 7000–400  $\text{cm}^{-1}$ , with a resolution of 2  $\text{cm}^{-1}$ . The spectra were recorded at least 24 h after changing the temperature of the water vapor source.

The Raman spectra excited by the laser beam of an argon Spectra Physic Laser Stabilité 2017 were collected on a Jobin-Yvon T64000 spectrometer equipped with an optical microscope, a 3-fold monochromator, and a nitrogen-cooled CCD camera. The laser beam at the 514.5-nm wavelength was focused with a long-frontal  $\xi 50$  objective (numerical aperture = 0.5) on an area of about 3  $\mu\text{m}^2$ . Ambient condition experiments at  $25 \pm 2$  °C were carried out by using a laser power on the sample of approximately 30 mW. Vacuum experiments were performed in a closed cell, related to a primary vacuum

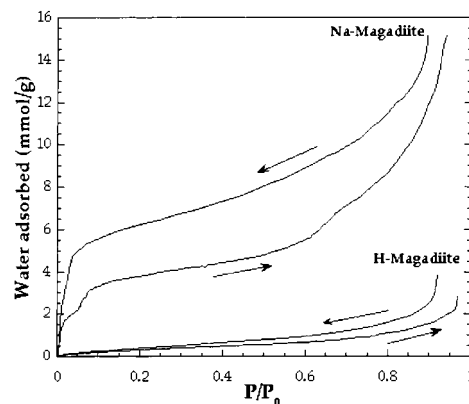


**Figure 1.** Water vapor adsorption–desorption isotherms at 30 °C of Na- and H-magadiite.

up to 1 Pa at a laser power of approximately 45 mW on the sample. The backscattered Raman spectra were collected in a confocal mode to avoid optical artifact. The spectral resolution was 3  $\text{cm}^{-1}$ , with a wavenumber precision better than 1  $\text{cm}^{-1}$ .

## Results

**Water Adsorption Gravimetry.** Figure 1 presents the water adsorption isotherms for Na- and H-magadiite. The curve obtained for Na-magadiite was presented and interpreted in a previous paper.<sup>30</sup> The difference in swelling behavior for these two layered silicates is clearly illustrated in this graph. The amount of water adsorbed for Na-magadiite is much higher than for H-magadiite. Assuming a cross-sectional area of 0.106  $\text{nm}^2$  for adsorbed water molecules,<sup>32</sup> the equivalent BET surface areas are around 190 and 17  $\text{m}^2\cdot\text{g}^{-1}$ , for Na- and H-magadiite, respectively, which confirms that, in contrast to the Na form, H-magadiite does not swell upon water adsorption.

**NMR Spectroscopy.** The <sup>29</sup>Si NMR MAS spectra and the corresponding cross polarization (CP) spectra of Na-magadiite, fully dehydrated Na-magadiite, and H-magadiite are shown in Figure 2. The data and calculated  $Q^3/Q^4$  ratios are summarized in Table 1. Na-magadiite exhibits, at least, four resonances at  $-99.1$ ,  $-109.6$ ,  $-111.1$ , and  $-13.7$  ppm. On the basis of chemical shifts, the  $-99.1$  ppm signal is assigned to Si atoms in a  $Q^3$  tetrahedral environment, i.e.,  $\text{HOSi}(\text{OSi})_3$  or  $\text{Na}^+[\text{OSi}(\text{OSi})_3]$ , and the other three bands are assigned to Si in a  $Q^4$  configuration, i.e.,  $\text{Si}(\text{OSi})_4$ . The CP method leads to an increase of the intensity of the  $Q^3$  signal and a decrease in intensity of the  $Q^4$  signal. When Na-magadiite is fully dehydrated, the signals of the <sup>29</sup>Si MAS NMR spectrum widen. The  $Q^3$  signal remains at about the same chemical shift as the hydrated sample, whereas the  $Q^4$  region is reduced to a single broad signal at  $-110.8$  ppm. The CP experiment yields two  $Q^3$  signals of increased intensity at  $-98.5$  and  $-100.7$  ppm and three  $Q^4$  signals at lower intensity with chemical shifts drifted toward lower values than those observed for the hydrated sample. In the case of H-magadiite, the <sup>29</sup>Si MAS NMR spectrum exhibits a  $Q^3$  signal at  $-101.7$  ppm and, at least, two  $Q^4$  signals at  $-111.7$  and  $-114.5$  ppm. As in the case of Na-magadiite sample, the CP experiment leads to an increase in intensity of the  $Q^3$  signal. An additional  $Q^4$  signal appears at  $-114.1$  ppm. The comparison between the MAS and CP MAS NMR spectra reveals a clear increase

(31) Pelletier, M.; de Donato, P.; Thomas, F.; Michot, L. J.; Gérard, G.; Cases, J. M. Clays for our future. In Proceedings of the 11<sup>th</sup> International Clay Conference, Ottawa, Canada, 1997; Kodama, H., Mermut, A. R., Torrance, J. K., Eds.; p 555.

(32) Hagymassy, J.; Brunauer, S.; Mikhail, R. S. H. *J. Colloid Interface Sci.* **1969**, *29*, 485.

(33) Grimmer, A. R.; Starke, P.; Wieker, W.; Mägi, M. *Z. Chem.* **1982**, *22*, 44.

(34) Bavière, A. Master of Science Thesis, Michigan State University, 1992.

(35) Dailey, J. S.; Pinavaia, T. J. *J. Inclusion Phenom. Mol. Recognit. Chem.* **1992**, *13*, 47.

(36) Lazarev, N. *Vibrational Spectra and Structure of Silicates*; Consultants Bureau: New York, 1972 and references therein.

(37) Huang, Y.; Jiang, Z.; Schwiager, W. *Microporous Mesoporous Mater.* **1998**, *26*, 215.

(38) Grimmer, A. R.; von Lampe, F.; Mägi, M.; Lippmaa, E. *Chem. Phys. Lett.* **1983**, *97*, 185.

(39) Smith, J. V.; Blackwell, C. S. *Nature* **1983**, *303*, 223.

(40) Ramdas, S.; Klinowski, J. *Nature* **1984**, *308*, 521.

(41) Grimmer, A. R. *Chem. Phys. Lett.* **1985**, *119*, 416.



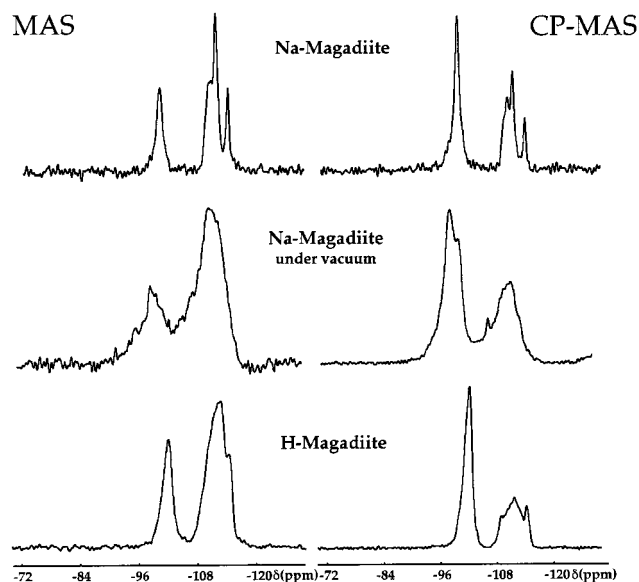


**Figure 2.**  $^{29}\text{Si}$  MAS NMR spectra of synthetic Na-magadiite and H-magadiite samples. On the left, the FT NMR spectra and, on the right, the CP NMR spectra are shown. All chemical shift values are given in ppm from liquid  $\text{Me}_4\text{Si}$ .

**Table 1.**  $^{29}\text{Si}$  MAS and CP-MAS NMR Chemical Shifts (ppm) and Calculated  $Q^3/Q^4$  Ratios for Na- and H-Magadiite

	MAS		CP-MAS		ratio $Q^3/Q^4$
	$Q^3$	$Q^4$	$Q^3$	$Q^4$	
Na-magadiite	-99.1	-109.6	-99.1	-109.7	0.4
		-111.1		-111.1	
		-113.7		-113.7	
Na-magadiite under vacuum	-98.8	-110.8	-98.5	-106.9	0.5
				-109.6	
				-112.0	
H-magadiite	-101.7	-111.7	-101.7	-109.0	0.4
		-114.5		-111.5	
				-114.1	

of the CP  $Q^3$  NMR signal for the three samples. Such a behavior is typical of samples with strong interactions between Si atoms  $Q^3$  and protons.<sup>33</sup> The  $Q^3/Q^4$  ratios of the three samples are presented in Table 1. Na- and H-magadiite exhibit similar values (0.4), whereas the ratio increases up to 0.5 in the case of dehydrated Na-magadiite. The chemical shifts and  $Q^3/Q^4$  ratios observed for magadiite are consistent with those reported by Bavière,<sup>34</sup> Dailey et al.,<sup>15,35</sup> and Almond et al.<sup>24</sup> Based on a systematic study of the influence of pulse delays on the experimental spectra, these authors<sup>15,24,35</sup> showed that pulse delays of at least 3 s were required for a correct determination of the  $Q^3/Q^4$  ratios. We then chose to use pulse delays of 5 s.

**Infrared Spectroscopy.** Figure 3 presents the evolution upon water desorption of the IR spectra of Na-magadiite in the 1400–500  $\text{cm}^{-1}$  range. This region displays the vibrations due to the silicate layer and charge-balancing cations. According to previous studies,<sup>28,36,37</sup> this spectrum can be discussed by splitting it into three parts. The first part (1400–950  $\text{cm}^{-1}$ ) concerns the antisymmetric stretching modes of Si–O–Si bridges,  $\nu_{\text{as}}(\text{Si–O–Si})$ , and the stretching modes of terminal Si–O– bonds,  $\nu(\text{Si–O–})$ . The second region (950–700  $\text{cm}^{-1}$ ) includes the symmetric stretching modes of Si–O–Si bridges,  $\nu_{\text{s}}(\text{Si–O–Si})$ . Between 700

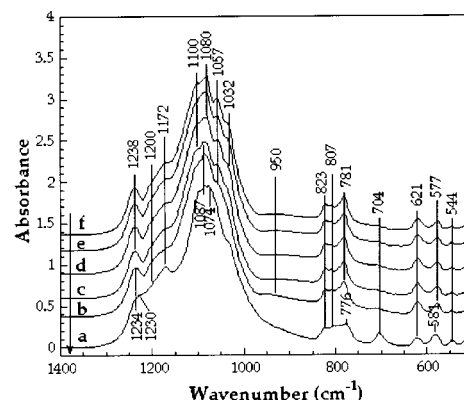


**Figure 3.** Evolution of infrared spectra (1400–500  $\text{cm}^{-1}$ ) of Na-magadiite at 30 °C upon water desorption. From a to f: under vacuum and  $P/P_0 = 0.010, 0.020, 0.030, 0.360,$  and  $0.440$ .

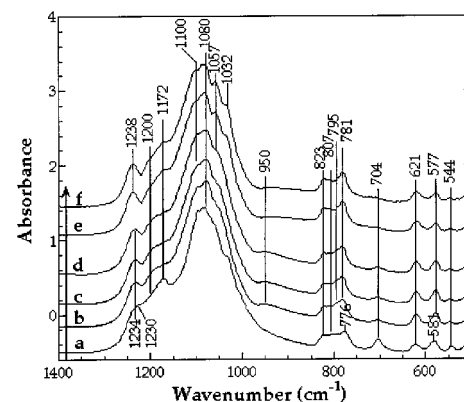


**Figure 4.** Evolution of infrared spectra (1400–500  $\text{cm}^{-1}$ ) of Na-magadiite at 30 °C upon water adsorption. From a to f: under vacuum and  $P/P_0 = 0.020, 0.030, 0.060, 0.300,$  and  $0.850$ .

and 400  $\text{cm}^{-1}$ , one can observe the phonon modes due to bending of Si–O–Si and O–Si–O ( $\delta\text{SiO}$ ).

In the first region, for  $P/P_0 = 0.440$ , one can observe bands at 1238, 1100, 1080, and 1057  $\text{cm}^{-1}$  and shoulders at 1172 and 1032  $\text{cm}^{-1}$ . Water desorption affects all these bands except the shoulder at 1032  $\text{cm}^{-1}$ . The 1238- $\text{cm}^{-1}$  band slowly decreases and shifts toward lower wavenumbers; under vacuum, it is reduced to a shoulder around 1230  $\text{cm}^{-1}$ . The profile of the massive around 1080–1100  $\text{cm}^{-1}$  changes. A component at 1087  $\text{cm}^{-1}$  appears from  $P/P_0 = 0.02$ . The shoulder at 1172  $\text{cm}^{-1}$  is only affected between  $P/P_0 = 0.01$  and vacuum, as its intensity increases markedly. The intensity of the 1057- $\text{cm}^{-1}$  band decreases upon water desorption and finally disappears under vacuum.

The second region exhibits bands at 823, 807, 781, and 704  $\text{cm}^{-1}$ . The intensity of the 781- $\text{cm}^{-1}$  band decreases upon water desorption. It decreases strongly and shifts to 776  $\text{cm}^{-1}$  when the sample is put under vacuum. In contrast, the shoulder at 704  $\text{cm}^{-1}$  becomes really marked under vacuum.

In the third region, three bands are observed at 621, 577, and 544  $\text{cm}^{-1}$ . Under vacuum, these three bands widen. The intensity of both the 544- and 577- $\text{cm}^{-1}$  bands increases and this latter band shifts to 581  $\text{cm}^{-1}$ .

Figure 4 presents the evolution upon water adsorption of the IR spectra of Na-magadiite in the 1400–500  $\text{cm}^{-1}$  region. As already observed in the ranges corresponding to water bending and stretching,<sup>30</sup> the patterns are

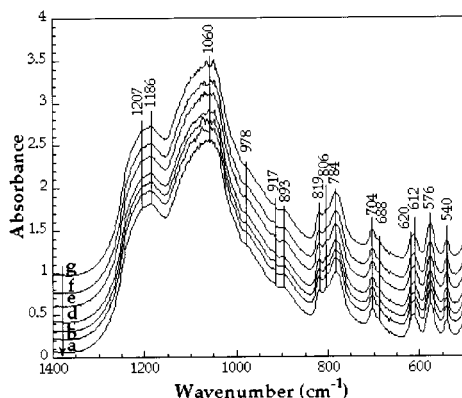


**Figure 5.** Evolution of infrared spectra (1400–500  $\text{cm}^{-1}$ ) of H-magadiite at 30 °C upon water desorption. From a to g: under vacuum and  $P/P_0 = 0.030, 0.060, 0.100, 0.260, 0.760,$  and  $0.850$ .

reversible as only marginal differences can be observed between spectra recorded in adsorption or desorption. Only two differences can be noted: (i) the band at 950  $\text{cm}^{-1}$  is present in adsorption for  $0.010 < P/P_0 < 0.060$ , whereas it is only remarkable for  $P/P_0 = 0.010$  in desorption, and (ii) around 800  $\text{cm}^{-1}$ , the evolution from three bands under vacuum to four bands in the presence of water vapor is more marked.

Figure 5 shows the evolution of infrared spectra of H-magadiite upon water desorption in the 1400–500  $\text{cm}^{-1}$  region. In the first region, absorptions are present at 1207, 1186, 1060, and 978  $\text{cm}^{-1}$ . Compared with Na-magadiite, the bands are shifted and the broad band around 1080  $\text{cm}^{-1}$  is much less clearly defined. In the second region, bands at 917, 893, 819, 806, 784, and 704  $\text{cm}^{-1}$  are noted. As in the first region, the band positions are systematically shifted from their positions in the sodium sample. Finally, in the third region, there is a shoulder at 688  $\text{cm}^{-1}$  and bands at 620, 612, 576, and 540  $\text{cm}^{-1}$  at wavenumbers close to what was observed on Na-magadiite. The most striking feature of these spectra compared to the case of Na-magadiite is their complete independence on the water content. This confirms the water adsorption results, which revealed that the interlayer region of H-magadiite was not accessible to water molecules for  $0 < P/P_0 < 0.85$ .

**Raman Spectroscopy.** The Raman spectra of Na-magadiite between 100 and 1300  $\text{cm}^{-1}$  are shown in Figure 6 for various hydration conditions. The highest hydration corresponds to the sample covered with a water drop. Only spectra in desorption will be presented, since measurements carried out after exposing the dehydrated sample to the atmosphere have revealed that the observed changes were fully reversible. As in the case of IR data, the Raman spectra will be divided into three regions.

In the first region, when Na-magadiite is fully hydrated, its Raman spectrum exhibits two small bands at 1240 (barely visible) and 1186  $\text{cm}^{-1}$  and a broad intense band at 1061  $\text{cm}^{-1}$ . Under atmospheric conditions, the bands at 1240 and 1186  $\text{cm}^{-1}$  fade, a sharp band at 1081  $\text{cm}^{-1}$  can be noticed, and the band at 1061  $\text{cm}^{-1}$  broadens. It must be pointed out that this spectra is coherent with the one described by Huang et al. except that we never observed a band at 992  $\text{cm}^{-1}$ .<sup>28</sup> For a residual pressure of 300 Pa, a shoulder at 1042

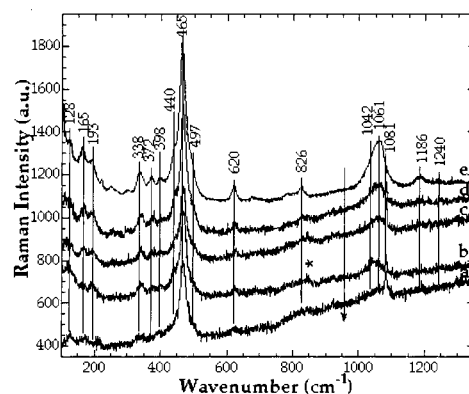


**Figure 6.** Evolution of Raman spectra (1300–100  $\text{cm}^{-1}$ ) of Na-magadiite at 25 °C upon desorption. From a to e:  $P = 0.9, 40,$  and  $300$  Pa, normal air conditions, and under water.

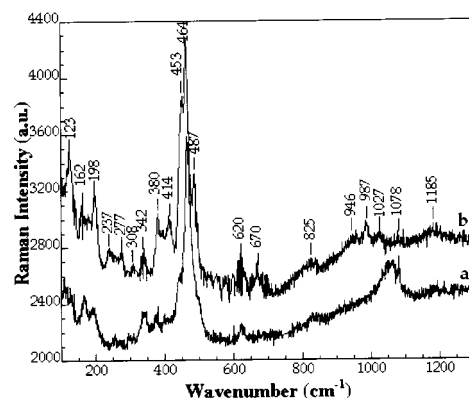


**Figure 7.** Raman spectra (1300–100  $\text{cm}^{-1}$ ) at 25 °C of (a) Na-magadiite in normal air conditions and (b) H-magadiite.

$\text{cm}^{-1}$  appears, which gets more marked under a residual pressure of 40 Pa. Finally, when the sample is under higher vacuum (0.9 Pa), only the sharp band at 1081  $\text{cm}^{-1}$  is clearly observable.

In the second region, a single band at 826  $\text{cm}^{-1}$  is observed and its intensity decreases with decreasing pressure (the band pointed with an asterisk in Figure 6 corresponds to a parasite signal due to the objective of the microscope).

In the third region, the spectra exhibits bands at 620, 465, 398, 372, 338, 193, 165, and 128  $\text{cm}^{-1}$  and shoulders at 497 and 440  $\text{cm}^{-1}$ . Upon pumping, the intensity of the bands at 620, 440, 372, 338, and 193  $\text{cm}^{-1}$  decreases, whereas all the other bands appear nearly unaffected by the water content in the sample.

Figure 7 displays a comparison between the Raman spectra of H-magadiite and Na-magadiite under ambient atmosphere. As observed by IR spectroscopy (Figure 5), pumping does not provoke any significant change in the spectra of H-magadiite. Differences between the two spectra can be noticed in the first and third regions. In the first region, additional bands are observed at 1027, 987, and 946  $\text{cm}^{-1}$ , whereas the band at 1061  $\text{cm}^{-1}$  disappears. In the third region, new bands clearly appear at 670, 487, 453, 414, and 380  $\text{cm}^{-1}$ .

## Discussion

As stated by many authors,<sup>3,21,24</sup> water molecules directly influence the structural features of magadiite. The use of three spectroscopic techniques under variable

**Table 2.**  $^{29}\text{Si}$  MAS NMR Chemical Shifts of Na- and H-Magadiite, with the Estimated Characteristic Mean Si–O–Si Bond Angle, Si–O Length, and Si–Si Length of the Corresponding  $Q^4$  Units

	$\delta Q^4$ , ppm	mean Si–O–Si, <sup>a</sup> deg	mean Si–O, <sup>b</sup> nm	mean Si–Si, <sup>c</sup> nm
Na-magadiite	-109.6	146.5	0.161	0.312
	-111.1	148.8	0.160	0.313
	-113.7	153.0	0.159	0.314
Na-magadiite under vacuum	-110.8	148.4	0.160	0.312
H-magadiite	-111.7	149.8	0.160	0.313
	-114.5	154.4	0.158	0.315

<sup>a</sup> Calculated using the relation  $\delta = -55.821 \cos(\text{Si-O-Si}) - 176.65$  ( $r^2 = 0.998$ ).<sup>39</sup> <sup>b</sup> Calculated using the relation  $\delta = (-0.222 \times 10^4)d(\text{Si-O}) - 446.3$  ( $r^2 = 0.917$ ).<sup>39</sup> <sup>c</sup> Calculated using the relation  $\delta = -392.10 - 1633.6d(\text{Si-Si}) - 176.65$  ( $r^2 = 0.994$ ).<sup>39</sup>

water contents indeed confirms such a statement and yields new constraints on the structural features of magadiite.

**Influence of Water on Crystallinity.** NMR data provide a first evidence that water losses are accompanied by a related decrease in the crystallinity of magadiite (Figure 2). This is proven by the broadening of the signals of Na-magadiite under vacuum or H-magadiite (which does not exhibit any significant uptake of interlayer water) when compared to the initial Na-magadiite. It is even more striking when the NMR chemical shifts are used for estimating the mean Si–O–Si bond angles, Si–O lengths, and Si–Si lengths of the corresponding  $Q^4$  units (Table 2).<sup>38–41</sup> When Na-magadiite is fully dehydrated, the number of observable Si environments is reduced from three to one, the broadening of the peak under vacuum conditions reflecting in increase in the local disorder at framework silicon sites. When sodium ions are totally exchanged by protons, Si environments are reduced to two, but  $Q^3/Q^4$  ratios remain equivalent, and even large bond angles are conserved. This proves that no bonds are broken and that for H-magadiite no opened bridges are formed. Dehydration as seen by the widening of  $^{29}\text{Si}$  NMR signals then just seems to induce some slight distortion of the initial Na-magadiite structure.

The decrease in crystallinity occurring upon dehydration is also evidenced by Raman experiments. Indeed, the spectrum obtained for Na-magadiite placed under water exhibits the thinnest scattered bands and a better signal-to-noise ratio. Diminishing water contents induces noisier signals. When the sample is put under strong vacuum (Figure 6a) all the bands are affected except the most intense band at  $465\text{ cm}^{-1}$ , due to vibrational modes of silicon–oxygen tetrahedra engaged in six-membered rings.<sup>28,42,43</sup>

The structural role of water in Na-magadiite is also confirmed by IR spectra. As shown in Figures 3 and 4, water desorption and adsorption provoke changes in the  $1100$  and  $800\text{ cm}^{-1}$  regions of the Na-magadiite spectra, i.e., in regions corresponding to Si–O–Si vibrations. The main features are a broadening of the bands in the domain centered around  $1080\text{ cm}^{-1}$ , which suggests a

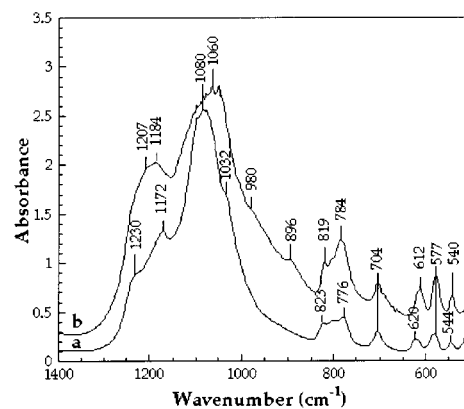


**Figure 8.** IR spectra ( $1400\text{--}500\text{ cm}^{-1}$ ) at  $30\text{ }^\circ\text{C}$  of (a) Na-magadiite under vacuum and (b) H-magadiite under vacuum.

lower crystallinity. The same conclusion is obtained from a comparison of the IR spectra of Na-magadiite and H-magadiite in the region  $1400\text{--}500\text{ cm}^{-1}$  (Figure 8).

**Influence of Water on the Layer/Cation Interactions.** The Raman spectrum of fully hydrated Na-magadiite (Figure 6, spectrum e) exhibits a broad band at  $1061\text{ cm}^{-1}$ . Under ambient conditions, an additional sharp signal appears at  $1081\text{ cm}^{-1}$  (Figure 6, spectrum d). A band at  $1064\text{ cm}^{-1}$  was also observed by Huang et al. who assigned it to the presence of both  $Q^3$  and  $Q^4$  species in Na-magadiite, suggesting a multilayer structure.<sup>28</sup> The evolution of this region with varying water contents brings new information about the precise assignment of these components. Indeed, upon pumping, a weak signal at  $1042\text{ cm}^{-1}$  becomes more distinguishable and is clearly observed for low water contents (Figure 6, spectra b and c). This component disappears when Na-magadiite is fully dehydrated, and at this stage, only the sharp  $1081\text{-cm}^{-1}$  signal remains. The Raman spectrum of H-magadiite (Figure 7) exhibits a band at  $980\text{ cm}^{-1}$  which can be assigned to the stretching vibrations of Si–OH groups. This band is associated with a component at  $487\text{ cm}^{-1}$  assigned to a kind of torsional mode of  $Q^3$  environments.<sup>44</sup> The spectrum does not exhibit any signals at  $1042$ ,  $1061$ , or  $1081\text{ cm}^{-1}$ ; the weak component around  $1080\text{ cm}^{-1}$  may be assigned to the vibrational mode  $\nu_{\text{as}}\text{ SiOSi}$  that gives rise to an intense IR absorption around  $1060\text{ cm}^{-1}$ . The bands around  $1100\text{ cm}^{-1}$  are associated with the stretching vibrations of the terminal nonbridging oxygens,  $\nu(\text{Si-O}^-)$ , in  $Q^3$  species.<sup>45–48</sup> Therefore, the three bands at  $1042$ ,  $1061$ , and  $1081\text{ cm}^{-1}$  can be assigned to layer/water/cation interactions. The  $1061\text{-cm}^{-1}$  component would then correspond to  $\text{Si-O}^-(\text{H}_2\text{O})_x\text{-Na}^+$ , the  $1042\text{ cm}^{-1}$  to a  $\text{Si-O}^-\text{H}_2\text{O-Na}^+$  association, and the  $1081\text{ cm}^{-1}$  to  $\text{Si-O}^-\text{Na}^+$ . The layer/water/cation interaction then clearly exhibits three distinct steps as a function of water content. It must be pointed out that the presence of these three hydration stages was already revealed when we studied the evolution of water vibra-

(44) Humbert, B.; Burneau, A.; Gallas, J. P.; Lavalley, J. C. *J. Non Cryst. Solids* **1992**, *143*, 75.

(45) Bates, J. B. *J. Chem. Phys.* **1972**, *56*, 1910.

(46) Bates, J. B. *J. Chem. Phys.* **1972**, *57*, 4042.

(47) Furukawa, T.; Fox, K. E.; White, W. B. *J. Chem. Phys.* **1981**, *75*, 3226.

(48) McMillan, P. *Am. Miner.* **1984**, *69*, 622.

(42) Sharma, S. K.; Simons, B.; Yoder, H. S. *Am. Miner.* **1983**, *68*, 113.

(43) Sharma, S. K.; Philpotts, J. A.; Matson, D. W. *J. Non Cryst. Solids* **1985**, *71*, 403.



tions in Na-magadiite as a function of water content.<sup>30</sup> The different water populations observed are then directly linked to changes in the position of the sodium cation with regard to the silicate layer. The evolution of the IR spectra upon water adsorption reveals some more information about the interaction between silicate layers and sodium cations clearly distinct from what is observed with some other layered silicates.<sup>49</sup> Indeed, as already mentioned, most changes occur in IR around  $1100\text{ cm}^{-1}$  ( $\nu_{\text{as}}\text{ SiOSi}$ ) and around  $800\text{ cm}^{-1}$  ( $\nu_{\text{s}}\text{ SiOSi}$ ), whereas bands near  $600\text{ cm}^{-1}$  remain mostly unaffected.

**Structural Considerations.** The differences observed between the IR and Raman spectra of Na-magadiite lead Huang and co-workers to the conclusion that this silicate is centrosymmetric, since the principle of mutual exclusion applies.<sup>28</sup> Still, it must be pointed out that exclusion does not univocally imply a centrosymmetric nature of the solid under investigation. On the basis of previous powder diffraction studies suggesting that this mineral belongs to the monoclinic crystal system,<sup>5,50</sup> Huang et al. proposed a  $C_{2h}$  point groups symmetry for magadiite. When looking at the IR and Raman spectra of Na-magadiite under ambient conditions, the differences between the two spectra are not striking, which would tend to suggest a noncentrosymmetric character for hydrated samples, opposite to what was proposed by Huang *et al.*<sup>28</sup> from their analysis of the IR and Raman spectrum of Na-magadiite.

A comparison of the same spectra under vacuum shows that a band at  $704\text{ cm}^{-1}$  is present only in the IR spectrum. The same feature is observed on H-magadiite where the  $704\text{ cm}^{-1}$  component exists only in IR. This band can be assigned to a  $\nu_{\text{s}}(\text{Si}-\text{O}-\text{Si})$  vibration which appears only when some coupling exists between adjacent silicate layers. Indeed, it is also observed for H-magadiite whose basal distance ( $11.8\text{ \AA}$ ) is very close to that observed for fully dehydrated Na-magadiite ( $12.1\text{ \AA}$ ).<sup>30</sup> The principle of mutual exclusion for the  $704\text{ cm}^{-1}$  component might then suggest that both dehydrated Na-magadiite and H-magadiite could bear a centrosymmetric character.

Under ambient conditions, Na-magadiite exhibits IR and Raman bands at  $1238$  and  $1240\text{ cm}^{-1}$ , respectively. Based on an analogy with some zeolites, Garcès et al. interpreted this band as indicating the existence of five-membered rings in the structure.<sup>27</sup> Such interpretation was recently supported by Huang et al.<sup>28</sup> However, this band does not appear clearly in the case of H-magadiite, which suggests that this component is strongly linked to sodium cations. Furthermore, its intensity and position depend on the water content (Figures 3 and 4). It could then be tentatively assigned to Si-O-Si vibrations affected by the sodium ion and its hydration sphere. In such assumption, upon dehydration, sodium ions get closer to Si-O-, the rings vibration modes are then modified because sodium ions disturb their angles: the  $1238\text{-cm}^{-1}$  band would then shift up to  $1230\text{ cm}^{-1}$  for a fully dehydrated sample. Therefore, five-membered rings, if they exist, are sensitive to water

contents, which suggests that they could be located mainly on the external surfaces of the crystallites.

Na-magadiite exhibits an IR band at  $1172\text{ cm}^{-1}$  and a shoulder at  $1200\text{ cm}^{-1}$ . Based on observations by Lazarev on pyrosilicates containing the  $\text{Si}_2\text{O}_7$  group,<sup>36</sup> Huang interpreted these two bands as corresponding to Si-O-Si linkages with  $180^\circ$  bond angles in the structure of Na-magadiite.<sup>28</sup> Upon decreasing water contents (Figures 3 and 4), these two components do not exhibit a parallel evolution as the  $1200\text{-cm}^{-1}$  one seems to disappear under vacuum, whereas the  $1172\text{-cm}^{-1}$  component is enhanced. On the contrary, the  $1200\text{-cm}^{-1}$  component follows the same evolution as the band around  $950\text{ cm}^{-1}$ . This latter component exhibits a slightly different behavior in desorption or adsorption (Figures 3 and 4): in desorption it is clearly observed only for  $P/P_0 = 0.010$ , whereas in adsorption, it is present for  $0.020 < P/P_0 < 0.060$ . It must then be assigned to a  $\delta(\text{Si}-\text{OH})$  influenced by the presence of water molecules. Therefore, the band at  $1200\text{ cm}^{-1}$  seems to be associated with water-dependent vibrations. The existence of linear Si-O-Si chains can then not be deduced from the presence of this component only.

Na-magadiite exhibits a Raman and IR band at  $621\text{ cm}^{-1}$ , which was attributed to an accidental degeneracy by Huang et al.<sup>28</sup> However, this band exists in both Na- and H-magadiite for all the studied hydration states (Figures 3–7). In some silicates,  $620\text{ cm}^{-1}$  is associated with three-membered rings. In the case of magadiite, this band exists even when Na-magadiite is under water (Figure 6e) and can then not be due to three-membered rings, which would definitely open in such hydration conditions.<sup>44,51</sup>

Table 3 summarizes all this information by listing the assignments of the observed IR and Raman data for both hydrated and dehydrated samples.

In terms of structure, magadiite definitely presents some six-membered rings, whereas the existence of five-membered rings and Si-O-Si chains cannot be proven unambiguously from spectroscopic data. It then appears that the proposed analogy with zeolite structures may not really apply to these layer silicates. It may be fruitful to compare the vibrational and NMR spectra of magadiite with those obtained for silica polymorphs.  $\alpha$ -Quartz presents a band at  $464\text{ cm}^{-1}$ , associated with a Si-O-Si bond angle of  $144^\circ$ .<sup>44,52</sup> Such a signal is also observed in Na- and H-magadiite. On the other hand, the NMR  $Q^4$  signal observed at  $-109.6\text{ cm}^{-1}$  is located at a position similar to what is observed in  $\alpha$ -cristobalite,<sup>46</sup> which exhibits a main Raman signal at  $426\text{ cm}^{-1}$ . Furthermore, the profile of the IR spectrum of H-magadiite reveals broad bands at  $1184$  and  $1060\text{ cm}^{-1}$  and a massive centered around  $800\text{ cm}^{-1}$  with components at  $819$  and  $784\text{ cm}^{-1}$  (Figure 8), which suggest some similarities with the TO-LO modes observed on amorphous silica.<sup>45,53</sup> All these features show that despite the differences observed, silica polymorphs could be used advantageously as structural analogues of magadiite.

(49) Bérend, I.; Cases, J. M.; François, M.; Uriot, J. P.; Michot, L.; Masion, A.; Thomas F. *Clays Clay Miner.* **1995**, *43*, 324.

(50) McAtee, J. L.; House, R.; Eugster, H. P. *Am. Miner.* **1968**, *53*, 2061.

(51) Burneau, A.; Humbert, B.; Barrès, O.; Gallas, J. P.; Lavalley, J. C. In *Advances in Chemistry*; Bergna, H., Eds. **1994**, 199.

(52) Wyckoff, R. W. G. In *Crystal Structures*; Interscience: New York, 1963.

(53) Galeener, F. L. *J. Non Cryst. Solids* **1982**, *49*, 53.

**Table 3. Vibrational Data (cm<sup>-1</sup>) and Their Assignments for Hydrated and Dehydrated Na-magadiite and H-magadiite**

Na-Magadiite				H-Magadiite		Assignment
I.R.		Raman		I.R.	Raman	
Hydrated	Dehydrated	Hydrated	Dehydrated			
1238 <sub>m</sub>	1230 <sub>vw</sub>	1240 <sub>vw</sub>		1207 <sub>sh</sub>	1185 <sub>m</sub>	ν <sub>as</sub> (Si-O-Si)
1200 <sub>sh</sub>		1186 <sub>m</sub>		1186 <sub>m</sub>		
1172 <sub>sh</sub>	1172 <sub>m</sub>					
1100 <sub>s</sub>	1087 <sub>s</sub>	1081 <sub>s</sub>	1081 <sub>s</sub>	1078 <sub>vw</sub>	1072 <sub>m</sub>	→ Si-O-Na <sup>+</sup>
1080 <sub>s</sub>	1074 <sub>s</sub>	1061 <sub>s</sub>		1060 <sub>s</sub>		→ Si-O(H <sub>2</sub> O) <sub>z</sub> -Na <sup>+</sup>
1057 <sub>m</sub>		1042 <sub>m</sub>				→ Si-O-H <sub>2</sub> O-Na <sup>+</sup>
1032 <sub>w</sub>				978 <sub>sh</sub>	987 <sub>s</sub>	ν <sub>s</sub> (Si-O-Si)
				917 <sub>sh</sub>	946 <sub>sh</sub>	
823 <sub>m</sub>	823 <sub>w</sub>	826 <sub>m</sub>		893 <sub>w</sub>	825 <sub>m</sub>	
807 <sub>w</sub>	807 <sub>vw</sub>			819 <sub>w</sub>		
781 <sub>m</sub>	776 <sub>w</sub>			806 <sub>sh</sub>		
	704 <sub>m</sub>			784 <sub>m</sub>		→ coupling of silicate layers
621 <sub>m</sub>	621 <sub>m</sub>	620 <sub>s</sub>	620 <sub>vw</sub>	704 <sub>m</sub>	670 <sub>m</sub>	δ <sub>as</sub> (Si-O-Si)
				688 <sub>sh</sub>	620 <sub>s</sub>	
				620 <sub>sh</sub>		
577 <sub>m</sub>	581 <sub>m</sub>			612 <sub>m</sub>		→ six-membered ring
544 <sub>w</sub>	544 <sub>m</sub>	497 <sub>sh</sub>	497 <sub>sh</sub>	576 <sub>s</sub>	540 <sub>m</sub>	
		465 <sub>vs</sub>	465 <sub>vs</sub>		487 <sub>s</sub>	
		440 <sub>sh</sub>			464 <sub>vs</sub>	
		398 <sub>w</sub>	398 <sub>w</sub>		433 <sub>s</sub>	
		372 <sub>m</sub>	372 <sub>m</sub>		414 <sub>s</sub>	δ SiO lattice modes
		338 <sub>s</sub>	338 <sub>w</sub>		380 <sub>s</sub>	
					342 <sub>s</sub>	
					308 <sub>w</sub>	
					277 <sub>m</sub>	
		193 <sub>sh</sub>			237 <sub>m</sub>	
		165 <sub>m</sub>	165 <sub>w</sub>		198 <sub>s</sub>	
		128 <sub>w</sub>	128 <sub>w</sub>		162 <sub>m</sub>	
					123 <sub>s</sub>	

### Conclusions

The combination of three spectroscopies under variable water content clearly reveals that, in the case of layered silicates such as magadiite, hydration water must be considered as a key structural component which influence cannot be neglected. Indeed hydrated Na-

magadiite is much more crystalline than either the dehydrated form or the proton-exchanged sample that does not incorporate water molecules in its interlayer region. The difference between Na- and H-magadiite then seems to be primarily linked to changes in water content, as NMR and Raman spectra revealed no significant framework alteration upon Na/H exchange.

More information can be obtained by following the evolution of IR and Raman spectra as a function of increasing or decreasing water content. Changes in the water-cation-layer interactions can be followed in parallel on the stretching and bending vibrations of water molecules and on Si-O-Si stretching vibrations. Three distinct hydration states are then clearly evidenced. From a structural point of view, our study also sheds new light on the presence of five-membered rings and silicate chains. Five-membered rings, if present, are sensitive to water content. The presence of Si-O-Si bond angles close to 180° cannot be deduced from the presence of a doublet around 1200 cm<sup>-1</sup>, as the intensities of the two components of the doublet evolve in opposite directions with water content. No definite conclusion about the presence of Si-O-Si chains can then be obtained from vibrational spectroscopic studies. Finally, on the basis of our vibrational spectroscopic study, H-magadiite and dehydrated Na-magadiite may be considered as centrosymmetric, as suggested by complementary electron diffraction measurements currently in progress. In contrast, hydrated Na-magadiite does not seem to be centrosymmetric, which again reveals the importance of water in the structure of this mineral.

**Acknowledgment.** We acknowledge Dr. Piotr Teke-ly (Laboratoire de Méthologie RMN, UPRES A 7042, Nancy I) for giving us access to a Bruker MSL 300 solid-state high-resolution NMR spectrometer.

CM001205+